frontiers | Frontiers in Earth Science

TYPE Original Research
PUBLISHED 31 January 2024
DOI 10.3389/feart.2024.1253632

Check for updates

OPEN ACCESS

EDITED BY
Chang Zhang,
Chinese Academy of Sciences (CAS), China

REVIEWED BY
Tong Hou,
China University of Geosciences, China
Zhenyu Zhang,
Chinese Academy of Sciences (CAS), China

*CORRESPONDENCE
Ankur Ashutosh,
ankurashutoshsingh@gmail.com

RECEIVED 05 July 2023
ACCEPTED 09 January 2024
PUBLISHED 31 January 2024

CITATION
Pattnaik J, Ashutosh A, Janaarthanan PA, Viljoen F, Srivastava RK and Ueckermann H (2024), Arc-related Alaskan type magmatism: evidence from pyroxenites associated with the Pakkanadu alkaline-ultramafic complex, Southern India.
Front. Earth Sci. 12:1253632.
doi: 10.3389/feart.2024.1253632

COPYRIGHT
© 2024 Pattnaik, Ashutosh, Janaarthanan, Viljoen, Srivastava and Ueckermann. This is an open-access article distributed under the terms of the Creative Commons Attribution License (CC BY). The use, distribution or reproduction in other forums is permitted, provided the original author(s) and the copyright owner(s) are credited and that the original publication in this journal is cited, in accordance with accepted academic practice. No use, distribution or reproduction is permitted which does not comply with these terms.

Arc-related Alaskan type magmatism: evidence from pyroxenites associated with the Pakkanadu alkaline-ultramafic complex, Southern India

Jiten Pattnaik[1,2], Ankur Ashutosh[2]*, P. A. Janaarthanan[2], Fanus Viljoen[1], Rajesh K. Srivastava[2] and Henriette Ueckermann[1]

[1]Department of Geology, University of Johannesburg, Johannesburg, South Africa, [2]Department of Geology, Institute of Science, Banaras Hindu University, Varanasi, India

Petrological and major-trace element mineral chemistry studies have been carried out on pyroxenites from the Pakkanadu alkaline-ultramafic complex from the southern India to understand their origin and nature of magma responsible for ultramafic magmatism in the area. Pyroxenites display cumulus texture and consist of clinopyroxenes (cpx) and amphiboles (amp) as dominant phases with a subordinate amount of apatite, biotite, ilmenite, magnetite, pyrite, sphene, and calcite. Mineral chemistry classifies cpx as augite and diopside, whereas amp falls under tremolite-actinolite and hornblende-actinolite fields. Cpx are alkaline to sub-alkaline in composition and Mg# - Al_2O_3 compositions suggest their crystallization under high-pressure conditions. A negative correlation between Mg# and TiO_2 in cpx suggests early crystallization of magnetite and pyrite; high Mg# (76–92) suggests its link with the Alaskan-type intrusions, which may be crystallized through fractionation-accumulation Processes. Tectonic discrimination diagrams for cpx argue for the magmatic emplacements under an arc-tholeiitic environment in a subduction zone setting. Amp mineral chemistry (high SiO_2 and low TiO_2) indicate as the products of hydrothermal alteration of clinopyroxenes. A Low Al/Si ratio in the cpx suggests their derivation from silica-oversaturated magma, whereas low-Ti contents reflect slow cooling rate of the magma. Positive Rb, Ba and U anomalies in the multi-element patterns of the cpx probably signifying varying degrees of hydrothermal alteration in the studied samples. However, consistent Nb-Ta depletion can also be attributed to an enriched mantle source of the magma from which pyroxenites were crystallized. Moreover, single-cpx geothermobarometry yielded a crystallization temperature of 905 to 911°C under moderate to high pressure of 3–9 kbar.

KEYWORDS

pyroxenite, alkaline ultramafic complex, Pakkanadu, Alaskan type, arc-tholeiitic environment, subduction zone, enriched mantle, Southern India

1 Introduction

Genesis of ultramafic magmatic rocks, particularly pyroxenites connected to ultramafic-mafic complexes, is always a subject of profound discussion as they may be explained through different theories (e.g., Downes, 2007; Xiong et al., 2014; Tilhac et al., 2017). In many cases, pyroxenites are thought to be responsible for chemical heterogeneity in the upper mantle and represent ancient oceanic crust which contributes to the formation and development of mantle-derived melts (e.g., Hirschmann and Stolper, 1996; Hirschmann et al., 2003; Kogiso et al., 2003; 2004; Sobolev et al., 2005; Lambart et al., 2012). Experimental results portray that pyroxenites may be formed as cumulates by intracrustal fractionation of primitive, mantle-derived arc melts (Kay and Kay, 1985; Muntener and Ulmer, 2006). Furthermore, a better understanding of the petrogenesis of arc-related pyroxenites could provide important constraints on the contribution of slab-derived components to mantle-wedge melts as the source of primary arc magmas (Kelemen, 1990; Kostopoulos and Murton, 1992; Hawkesworth et al., 1993; Bernard and Ionov, 2013).

There are several theories known to explain the genesis of ultramafic (pyroxenite/peridotite) complexes. Medaris et al. (1995) have linked genesis of garnet-pyroxenite with the subduction of oceanic plate that tempted them to form as high-pressure crystal segregates from silicate magmas that originated in the asthenosphere and travel up to the lithosphere. Many connected genesis of ultramafic complexes are with the Alaskan-type layered intrusions, which are formed within subduction zones; they may have varying contributions from the subducted slab in arc to backarc settings (e.g., Helmy and El Mahallawi, 2003; Batanova et al., 2005; Helmy et al., 2014). Layered intrusions are thought to be the relics of basaltic magma chambers and constitute a potentially strong tool for decoding the geochemical development of magmas, probing magma chamber filling histories, and comprehending the various mechanisms connected to the solidification of the shallow crust. They often form in anorogenic tectonic settings along with large igneous provinces and considerable mantle partial melting (O'Driscoll and VanTongeren, 2017). Noble (1960) and Taylor (1960) identified the mafic-ultramafic complexes in southern Alaska as a unique class of intrusions, and Irvine (1974) termed them Alaskan-type. Since then, several unique complexes and belts of Alaskan-type mafic-ultramafic intrusions from orogenic belts or modern arc settings have been found globally. Alaskan-type mafic-ultramafic complexes are formed by crystal fractionation and mineral concentration processes and mostly display concentric features, which are likely to be formed in subduction related settings. Although, pyroxenites are discovered in supra-subduction zone environments (McInnes et al., 2001; Garrido et al., 2007; Jagoutz et al., 2007; Bouilholet al., 2011, 2015), however there are a few comprehensive petrological investigations on them from the Indian subcontinent (Sharma et al., 2019).

Pyroxenites have been documented from different cratons and mobile belts in the Indian Shield (e.g., Rao and Raman, 1979; Kutty et al., 1986; Srivastava and Sinha, 2007; Samuel et al., 2014; Renjith et al., 2016). They generally occur as xenoliths or ultramafic massifs or as number of mafic-ultramafic complexes reported in the Granulite Terrane of the southern India, mostly confined to the Cauvery Suture Zone (CSZ) (Figures 1A, B). The prominent ones include i) Salem mafic-ultramafic complex (SMUC), ii) Thenmudiyanur mafic-ultramafic complex (TMUC), iii) Sittampundi anorthosite complex (SAC), and iv) Pakkanadu ultramafic complex (PUC) (Figure 1B). The PUC is the part of the Pakkanadu alkaline-ultramafic complex (PAUC) (*cf.* Renjith et al., 2016; Srivastava et al., 2022) and it hosts several mafic-ultramafic rocks including serpentinized dunite, peridotite, pyroxenite, hornblendite, amphibolite, mafic granulite, charnockite, migmatite gneiss, etc., however pyroxenites dominate over others.

The PAUC, together with other alkaline-carbonatite complexes associated with the Dharmapuri rift zone (DRZ) (see Figure 1B), is supposed to be derived from a metasomatism induced enriched subcontinental lithospheric mantle (EM-I type mantle) beneath granulite terrane (*cf.* Kumar et al., 1998; Schleicher et al., 1998; Pandit et al., 2002; Srivastava et al., 2022). Many have studied the PAUC, particularly associated alkaline-carbonatite rocks (e.g., Schleicher et al., 1998; Moller et al., 2001; Pandit et al., 2002; Bhagat et al., 2021; Srivastava et al., 2022), however very less attention has been given to the associated pyroxenite rocks in the PUC.

Although, Sukumaran (1987) suggested that pyroxenites (and dunites), associated to the PAUC, are cumulates and derived from an alkali peridotite source; however no definite genesis is established. There is no detailed petrological and geochemical characterization of pyroxenites of the PUC available; hence, their genetic aspects are still unclear. This work presents a detailed study of field relationships, petrography, and first major-trace mineral chemistry of Pakkanadu pyroxenites to understand genesis and evolution of pyroxenites associated to the PAUC. This will also help to identify its likely genetic relationship with the other coeval rocks along the DRZ. There is no trace element study of clinopyroxenes from any ultramafic complex located along the DRZ, hence this is the first report of such a dataset.

2 Geological setting

The southern part of the Indian Shield is a well-known geological province comprising poly-metamorphic crustal blocks that collided together over a period ranging from the Neoarchean to the Neoproterozoic-Cambrian (Santosh et al., 2009; Collins et al., 2014). It is a wedge-shaped granulite terrain that terminates the Indian peninsula in the south and separated from the Dharwar craton by Fermor line in the north (e.g., Naqvi and Rogers, 1987; Ghosh et al., 2004). This terrain has been further divided into Northern Granulite Terrane (NGT) and the Southern Granulite Terrain (SGT) and the E-W trending Palghat-Cauvery Shear Zone (PCSZ) as the boundary which separates them (see Figures 1A, E.g.; Drury et al., 1984; Ramakrishnan, 1988; 1993; Ramakrishnan and Vaidyanadhan, 2010). The transition between the non-charnockitic cratonic terrain (amphibolite facies) in the north and the mobile belt of charnockitic rocks (granulite facies) in the south is marked by a tectonic zone called Salem block, which is characterized by extensive faulting and thrusting (Swaminath et al., 1974; Condie et al., 1982). Stretching from the southern boundary of the Dharwar craton to the PCSZ, it is typified by the presence of orthogneisses, metasedimentary rocks in the form of migmatites, charnockites, and granitoids (Bhaskar Rao, 2003; Clark et al., 2009; Saitoh et al., 2011).

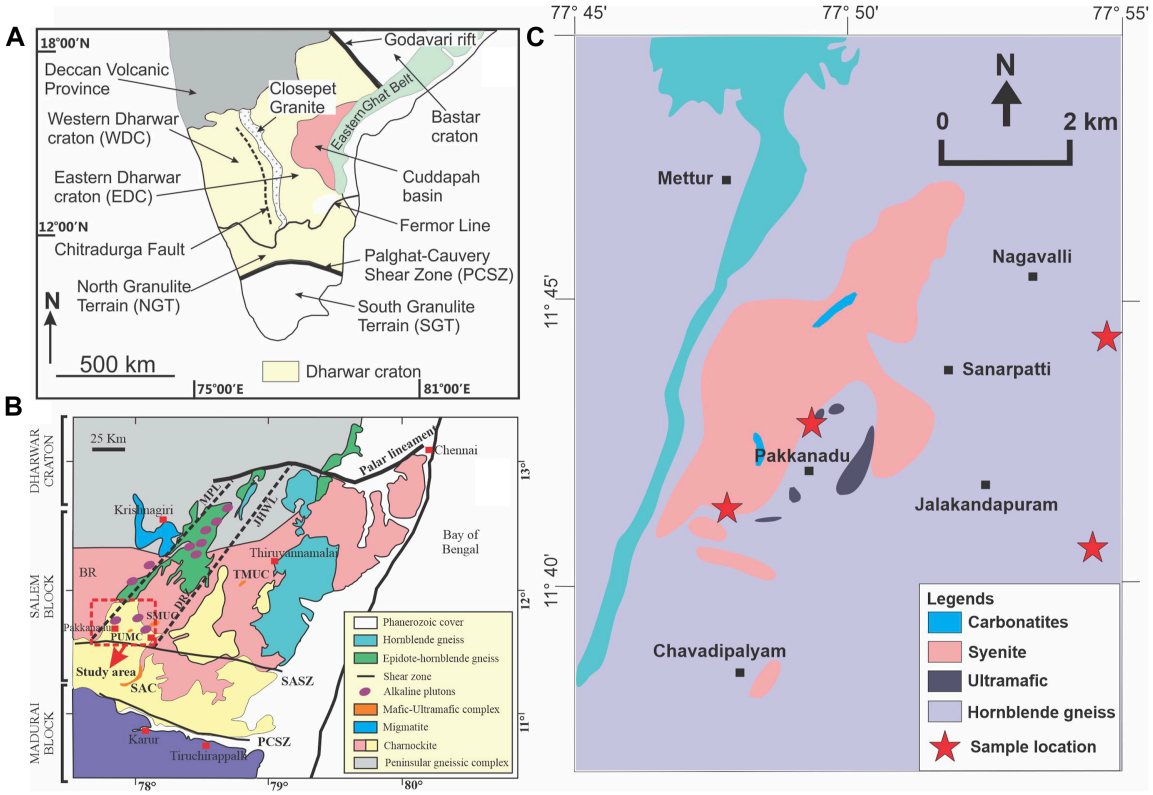

FIGURE 1
(A) Simplified geological map of the southern Indian Shield showing division of the Dharwar craton into different segments (*cf.* Geological Survey of India, 1994; Samal et al., 2021); **(B)** Geological map of western part of the Northern Granulite Terrane (NGT), southern India (modified after Srivastava et al., 2022). Dashed lines mark the boundaries of the Dharmapuri Rift Zone (DRZ) (after Gopalakrishnan, 2001; Chetty, 2017). Approximate locations of alkaline plutons are also shown (after Renjith et al., 2016). Abbreviations used: JHWL- Jawadi hill west lineament, MPL- Mettur Palakkadu lineament, PCSZ- Palaghat Cauvery Shear Zone, PUMC- Pakkanadu Ultramafic Complex, SAC- Sittampundi Anorthosite Complex, SASZ- Salem Attur Shear Zone, SMUC- Salem Mafic-Ultramafic complex, and TMUC- Thenmudiyanur Mafic-Ultramafic complex. Red rectangle shows location of study area; **(C)** Geological map of the Pakkanadu alkaline-ultramafic complex (modified after Bhagat et al., 2021).

The DRZ in the Salem Block (Figure 1B) underwent two stages of evolution (Gopalakrishnan, 1993); the first stage involved collisional tectonic setting that resulted in the suturing and welding of two crustal blocks on either side of DRZ, whereas the second stage was a rifting tectonic phase that began with the reactivation of shear zones and the development of a tensional fracturing system along NNE-SSW, N-S, and ENE-WSW directions. The latter phase of rifting was also associated with the emplacement of Neoproterozoic alkaline plutons. These alkaline plutons were emplaced along the DRZ within epidote hornblende gneiss (Renjith et al., 2016). The Dharmapuri alkaline-ultramafic province, consisting of carbonatites, syenites, lamprophyres, pyroxenites, and dunites, is approximately 700–800 million years old (Cryogenian) (e.g., Kumar et al., 1998; Schleicher et al., 1998; Miyazaki et al., 2000), therefore the age of the aborted Dharmapuri rift could be Neoproterozoic. This rifting could probably be due to the (Neoproterozoic) southward subduction of the Mozambique Ocean under the Madurai block causing extensional forces in the Salem block (Santosh et al., 2014). This passive mode of rifting within the Salem block-initiated upwelling of asthenosphere, subsequent intruding into the sub-continental lithospheric mantle (SCLM).

The Pakkanadu alkaline-ultramafic complex (PAUC) extends to about 35 km WNW of Salem town in Edappadi block of Salem district of Tamil Nadu. It mainly comprises of ultramafic rocks such as pyroxenites and dunites, carbonatites, migmatitic gneiss and syenites (Figure 1C). Carbonatitic intrusions are also reported within the pyroxenite bodies, mostly concordant fracture-fill, and diatremes (Pandit et al., 2002) (Figure 1C). Cpx exhibit hydrothermal alteration to amphiboles (amp) whereas the dunites are heavily serpentinized and are cut by asbestos and magnesite veins. Field relationship of the studied pyroxenite occurrences along DRZ is well established (e.g., Pandit et al., 2002; Renjith et al., 2016). The rifting and magma formation in the DRZ produced a diverse range of magmatic suites such as syenitoids, pyroxenite, dunite, carbonatite, and lamprophyres. Different magma batches, such as syenite, pyroxenite, and carbonatite, were created from their individual origins and deposited as alkaline intrusive complexes in the DRZ. The presence of intrusive cross-cutting relationships between syenite, pyroxenite, and carbonatite suggests that these litho units were emplaced as discrete magma batches rather than as differentiated products of a single magma. Pyroxenite was the first rock type to form, followed by syenite, and carbonatite was the final rock type to form. This

emplacement sequence is seen in all the DRZ's alkaline complexes (Renjith et al., 2016).

3 Methods

3.1 Scanning electron microscope (SEM)

The polished thin sections of Pakkanadu pyroxenites were coated with a 20 ηm thin layer of carbon using carbon coater (LEICA–EM ACE200) for scanning electron microscopy studies at the DST-SERB National Facility, Department of Geology, Banaras Hindu University, India. Several mineral phases like cpx, amp, Fe oxides, sphene, apatite, calcite, and pyrites along with their textures and chemical zoning (if any) were identified under Carl Zeiss RESEARCH EVO 18 scanning electron microscope (SEM) using an energy dispersive spectrometer. The backscattered electron images were also acquired for these mineral phases.

3.2 Electron probe micro analyzer (EPMA)

Major element compositions of the constituent minerals, particularly cpx and amp, were determined by EPMA using a Cameca SX-Five wave-length dispersive spectrometry (WDS) at the DST-SERB National Facility, Department of Geology, Banaras Hindu University, India. The polished thin sections were coated with a 20 nm thin layer of carbon for electron probe microanalyses using the LEICA-EM ACE200 instrument. The diameter of the beam was about 1 μm. The instrument with SX-Five software was run at an acceleration voltage of 15 kV and a beam current of 20 nA. The electron gun was fired with a LaB_6 source for generating the electron beam. Counting times were 30 s on the peak and 15 s on both left and right backgrounds. Natural andradite was used as an internal standard to verify the positions of crystals (SP1-TAP, SP2-LiF, SP3- LPET, SP4-LTAP, and SP5-PET) for corresponding wavelength dispersive (WD) spectrometers in the Cameca SX-Five instrument. The following X-ray lines were used in the analyses: Na-*Kα*, Mg-*Kα*, Al-*Kα*, Si- *Kα*, Ca-*Kα*, Ti-*Kα*, Cr-*Kα*, Mn-*Kα*, and Fe-*Kα*. Routine calibration, acquisition, quantification, and data processing were carried out using Sx SAB version 6.1 and SX-Results software of Cameca. X-PHI matrix correction is applied to the whole experimental work. The precision of the analysis is better than 1%. The representative major element compositions (in wt%) of the cpx and amp are represented in Tables 2, 3 respectively. The individual point analyses of each sample of the cpx and amp grains are provided in the Supplementary Tables S1, S2, respectively.

3.3 Laser ablation inductively coupled plasma mass spectrometry (LA-ICPMS)

Trace element analysis of the cpx was obtained by LA-ICPMS at the Spectrum facility of the University of Johannesburg, South Africa. A 193 nm ArFRESOlution SE Excimer Laser (formerly Australian Scientific Instruments, Fyshwick; currently Applied Spectra, Sacramento) was coupled to a Thermo Fisher iCAP RQ ICP-MS. A laser spot size of 80 μm, beam energy of 6 mJ, and a beam attenuation of 25% was used at a repetition rate of 10 Hz to achieve on-sample fluence of 1.9 J/cm^2. Ablations were done in a Laurin Technic dual-volume cell under a helium atmosphere with a He flow of 0.35 L/min, which was mixed with argon nebulizer gas at a flow rate of 0.8 L/min. N_2 gas at a flow rate of 1 L/min was added to the laser signal before entering the ICPMS to improve signal intensity. Analyte intensities were optimized before analyses while ensuring an oxide ratio below 1%. NIST612 standard glass was used as the bracketing standard, with ^{29}Si used as the internal standard. NIST610 and USGS reference glass BCR2G were used as secondary standards to evaluate the accuracy of results. Sets of 10 sample spots were bracketed by NIST612 analyses, along with NIST610, BCR2G, and JJ1424 (cpx mineral standard) as secondary standards. This allowed regular monitoring of accuracy and reproducibility. Accuracy and reproducibility were estimated from repeat analyses of the NIST610 as an unknown during the analytical sessions. The reproducibility was calculated from repeat measurements of the NIST610 reference glass, BCR2G and JJ1424 and were found to be <6%. The GLITTER software package (Van Achterbergh et al., 2001) was used for data reduction and processing. The trace element compositions (in ppm) of the cpx are represented in Table 2. The raw data of the trace elements of the clinopyroxenes along with the standards for reference are represented in the Supplementary Table S3.

4 Results

A total of nine fresh samples from the pyroxenite exposures were collected for the present study (see Table 1). Later, after careful petrographic examinations, out of the 9 samples, 4 samples were selected for the detailed studies (see red stars in Figure 1C).

TABLE 1 List of samples along with their geographic coordinate locations.

Sl. No.	Sample	Latitude (N)	Longitude (E)
1	PKD 22/1	11°42′02.4″N	77°50′32.6″E
2	PKD 22/2	11°42′23.3″N	77°49′23.8″E
3	PKD 22/3	11°41′12.3″N	77°47′51.6″E
4	PKD 22/4	11°42′55.5″N	77°54′59.6″E
5	PKD 22/5	11°43′54.9″N	77°55′15.9″E
6	PKD 22/6	11°43′58.4″N	77°55′22.3″E
7	PKD 22/6b	11°43′59″N	77°55′21″E
8	PKD 22/7	11°40′11.9″N	77°53′43″E
9	PKD 22/8	11°40′12.6″N	77°54′26.5″E

TABLE 2 Representative major (in wt% oxides) and trace element (in ppm) contents of pyroxenes along with estimated pressures and temperatures of the studied samples.

Trace elements	PKD 22/2	PKD 22/3	PKD 22/6	PKD 22/8
SiO_2	54.78	55.24	54.31	54.25
TiO_2	0.05	0.03	0.04	0.05
Al_2O_3	0.27	0.37	1.20	1.51
Cr_2O_3	0.04	0.03	0.02	0.04
FeO	2.71	7.05	7.04	6.94
MnO	0.13	0.09	0.03	0.09
MgO	16.82	14.05	13.39	12.55
CaO	24.54	21.82	22.16	22.48
Na_2O	0.32	1.44	1.50	0.83
K_2O	0.02	0.01	0.01	0.01
TOTAL	**99.69**	**100.14**	**99.68**	**98.74**
Cations based on 6 oxygens Cations				
Si	2.00	2.03	2.040	2.01
Ti	0.00	0.00	0.00	0.00
Al	0.01	0.02	0.07	0.05
Cr	0.00	0.22	0.00	0.00
Fe	0.08	0.00	0.22	0.22
Mn	0.00	0.77	0.00	0.00
Mg	0.92	0.86	0.70	0.74
Ca	0.96	0.10	0.91	0.88
Na	0.02	0.00	0.06	0.11
K	0.00	0.00	0.00	0.00
TOTAL	**4.00**	**4.00**	**4.00**	**4.00**
Wo	48.00	43.00	45.12	43.85
En	45.80	38.50	35.16	36.85
Fs	3.80	9.70	10.91	8.81
Mg#	**91.70**	**78.00**	**76.32**	**77.01**
Trace elements				
Li	6.073	2.970	2.754	1.072
Be	0.319	6.141	0.439	0.207
Al	7860.336	9887.564	16296.856	9381.389

(Continued on the following page)

TABLE 2 (*Continued*) Representative major (in wt% oxides) and trace element (in ppm) contents of pyroxenes along with estimated pressures and temperatures of the studied samples.

Trace elements	PKD 22/2	PKD 22/3	PKD 22/6	PKD 22/8
Si	249378.884	258727.681	254310.446	240170.384
Sc	76.582	58.062	57.619	18.247
Ti	1387.805	810.714	913.364	301.477
V	59.755	39.400	183.719	49.650
Cr	422.241	296.203	2382.974	570.243
Mn	1475.315	1387.841	1096.874	914.597
Co	43.046	58.380	67.559	58.520
Ni	147.259	184.015	388.392	447.184
Cu	0.541	0.328	0.319	0.394
Zn	42.353	104.611	97.830	61.058
Ga	3.397	4.680	5.281	3.099
Rb	0.392	0.298	0.303	0.061
Sr	486.417	212.850	71.984	22.620
Y	12.417	3.806	6.985	3.293
Zr	11.979	7.336	2.280	3.607
Nb	0.151	3.306	0.283	0.037
Cs	0.046	b.d.l	0.007	0.005
Ba	2.376	3.051	1.608	0.928
La	5.169	0.972	0.895	0.168
Ce	20.508	3.953	3.908	1.468
Pr	3.905	0.745	0.770	0.425
Nd	19.479	3.681	4.135	2.588
Sm	5.309	1.213	1.376	0.786
Eu	1.579	0.436	0.434	0.144
Gd	4.501	1.096	1.462	0.728
Tb	0.568	0.145	0.224	0.106
Dy	2.746	0.720	1.282	0.585
Ho	0.506	0.129	0.269	0.121
Er	1.179	0.294	0.690	0.316
Tm	0.150	0.040	0.095	0.047
Yb	0.872	0.240	0.583	0.281

(Continued on the following page)

TABLE 2 (*Continued*) Representative major (in wt% oxides) and trace element (in ppm) contents of pyroxenes along with estimated pressures and temperatures of the studied samples.

Trace elements	PKD 22/2	PKD 22/3	PKD 22/6	PKD 22/8
Lu	0.131	0.040	0.096	0.044
Hf	0.645	0.332	0.223	0.123
Ta	0.001	0.001	0.014	0.002
Pb	2.961	6.481	1.151	0.309
Th	0.042	0.003	0.004	0.015
U	0.044	0.004	0.003	0.005
P (Kbar)	3.48	5.77	8.61	7.31
T (°C)	906	905	911	905

Bold values indicate the "sum or total".

4.1 Petrography

The pyroxenites are coarse-grained and are composed predominantly of cpx (diopside and augite), amp, and Fe-Ti oxides.

Cpx are subhedral in shape with a prismatic habit and are pale green in color. They are extensively fractured and exhibit high relief. The amp found at the cpx grain boundaries are most likely secondary in nature (Figures 2C, D), and might have developed as a result of the deuteric alteration (uralitization). It suggests that a moderate degree of alteration affected the samples; however, their igneous texture is intact. The amp exhibit subhedral shape along with prominent 2-set cleavage and are secondary in nature (Figures 2E, F). The samples also contain 3%–4% opaque phases which are probably Fe-Ti oxides (ilmenites).

4.2 Scanning electron microscope (SEM) studies

Back scattered electron (BSE) images, along with their semi-quantitative energy-dispersive spectra (EDS) data were obtained (Figures 3, 4). Based on the EDS data, the mineral phases like cpx, hornblende, apatite, sphene, calcite, ilmenite, biotite, magnetite, and pyrite were identified in the studied pyroxenites (Figure 3). The BSE images clearly show the alteration of cpx to amp by reaction replacement as well (see Figure 4). BSE studies and EDS data suggest existence of iron-oxide (magnetite) and iron-sulphide (pyrite) together; this could possibly be inferred as a replacement of magnetite by pyrite due to hydrothermal alteration. The presence of other accessory phases like ilmenite (Figures 3C, E), calcite (Figure 3C), apatite (Figure 3D), biotite (Figure 3F), and sphene (Figure 3C) were also identified.

4.3 Mineral chemistry

The mineral chemistry of cpx and amp present in these pyroxenite samples were analysed. Major elements were analysed for cpx and amp, whereas trace elements were done only for cpx and is represented in Tables 2 and 3.

TABLE 3 Representative major element concentrations (in wt% oxides) of amphiboles in the studied pyroxenite samples.

Major oxides	PKD 22/2	PKD 22/3	PKD 22/6	PKD 22/8
SiO_2	53.76	55.76	55.25	54.82
TiO_2	0.33	0.12	0.13	0.03
Al_2O_3	3.93	1.81	2.50	3.82
FeO	5.07	7.53	7.51	6.25
MnO	0.13	0.12	0.10	0.04
MgO	20.48	19.12	19.10	19.65
CaO	12.39	11.19	12.66	12.83
Na_2O	1.79	1.65	0.54	0.67
K_2O	0.14	0.23	0.06	0.10
Total	**98.26**	**97.54**	**97.37**	**98.21**
Cations based on 23 oxygen atoms				
Si	7.50	7.83	7.74	7.62
Ti	0.03	0.01	0.01	0.00
Al	0.65	0.31	0.41	0.63
Fe	0.59	0.86	0.88	0.73
Mn	0.02	0.02	0.01	0.01
Mg	4.26	4.05	3.99	4.07
Ca	1.85	1.68	1.90	1.91
Na	0.48	0.47	0.15	0.18
K	0.02	0.04	0.01	0.02
TOTAL	**15.40**	**15.35**	**15.11**	**15.16**
Mg#	**87.81**	**82.55**	**81.92**	**84.86**

Bold values indicate the "sum or total".

4.3.1 Major-element geochemistry

Clinopyroxene: The MgO content in cpx ranges from 12.55 to 16.82 wt% and are relatively rich in Ca (Wo_{43-48}) whereas poor in Ti and Cr. The Mg# [Mg/(Mg+Fe)*100] ranges from 76 to 92. They fall in the diopside field (Figure 5A) on the pyroxene classification diagram (Morimoto et al., 1988). The Al_2O_3 vs. SiO_2 plot (Figure 5B) shows that they are non-alkaline in nature (Le Bas, 1962) and the Mg# vs. Al_2O_3 (Figure 5C) bivariate plot suggests that they are crystallized under high-pressure conditions (Medaris, 1972).

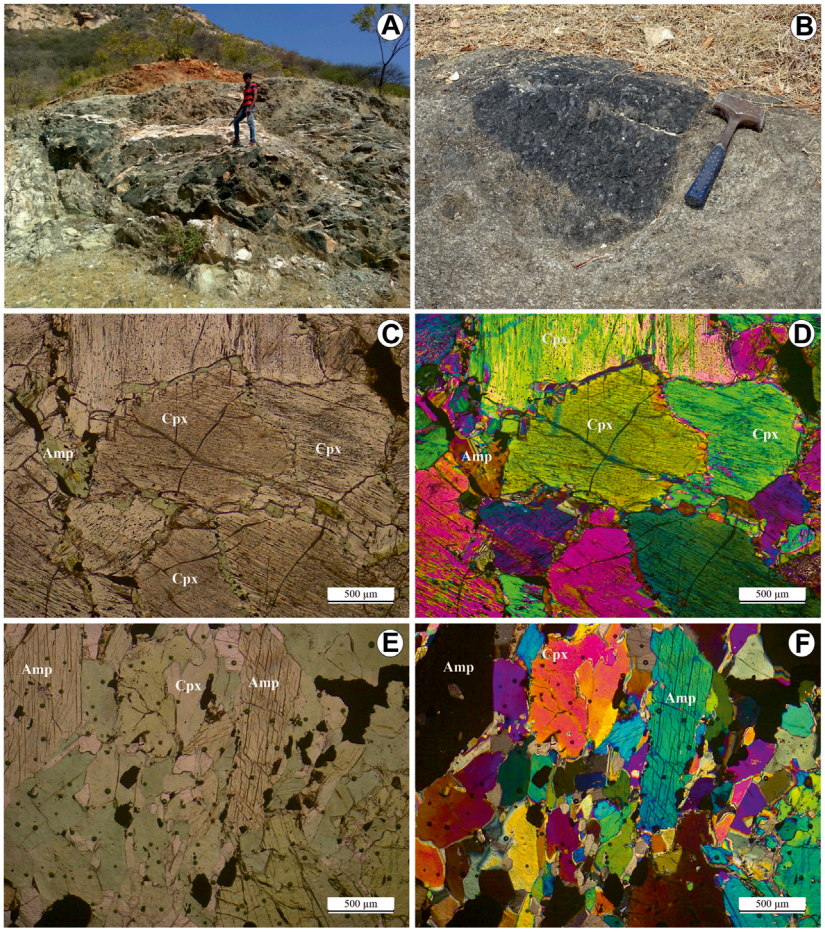

FIGURE 2
Field photographs showing **(A)** pyroxenite body from the Pakkanadu alkaline-ultramafic complex **(B)** pyroxenite occurring in the carbonatite-mica schist rock; Photomicrographs of the studied pyroxenite samples displaying cumulate texture; both in plane-polarized light **(C,E)** and cross-polarized light **(D,E)**. Abbreviations used: Clinopyroxene (Cpx), Amphibole (Amp).

Amphibole: They exhibit high MgO (19.10–20.48 wt%), high Al_2O_3 (1.81–3.93 wt%) and lower CaO (11.19–12.83 wt%) contents compared to cpx. The Mg# ranges from 81 to 88, almost similar to those in cpx. High SiO_2 (53.76–55.76 wt%) and low TiO_2 (0.03–0.33 wt%) contents indicate that they are the products of hydrothermal alteration of clinopyroxenes. In the Si vs. Mg# plot (Figure 5D), they fall in the tremolite-actinolite field and hornblende-actinolite fields (Leake et al., 1997).

4.3.2 Trace-element geochemistry of clinopyroxene

In the primitive mantle-normalized spider diagram (Figure 6A), a strong negative Ti- and Zr-anomalies have been observed in all samples, however, there is a low to moderate negative anomaly in Hf. Sr shows positive anomaly in all samples. Furthermore, PKD 22/2 and PKD 22/8 reflect negative Nb-anomaly whereas, PKD 22/3 and PKD 22/6 exhibit positive Nb-anomaly. The chondrite-normalized rare earth element (REE) pattern of cpx (Figure 6B) of three samples (PKD 22/2, PKD 22/3, and PKD 22/6) are sub-parallel to each other and exhibit negligible to moderate enrichment in Light-REE with slightly depleted Heavy-REE. The LREE/HREE ratio $(La/Yb)_N$ for PKD 22/2 and PKD 22/3 is 2.05 and 4.07, whereas, for PKD 22/6, the ratio is nearly 1. In contrast, sample PKD 22/8 displays depletion in LREE compared to HREE with $(La/Yb)_N$ ratio of 0.13; this also shows a significant negative Eu-anomaly (Eu/Eu*= 0.4–0.6). The other three samples do not show such anomaly (Eu/Eu*= 0.92–1.15). However, a uniform enrichment in Middle-REE with respect to HREE has been observed for all the samples having $(Gd/Yb)_N$ values ranging from 1.39 to 4.17.

4.4 Geothermobarometry

The chemical composition of pyroxene in igneous rocks varies widely in composition from intermediate to ultramafic, which is sensitive to the change in pressure and temperature of magmatic systems (e.g., Mercier, 1980; Nimis, 1995; Putirka et al., 1996; Nimis and Ulmer, 1998; Nimis, 1999; Nimis and Taylor, 2000;

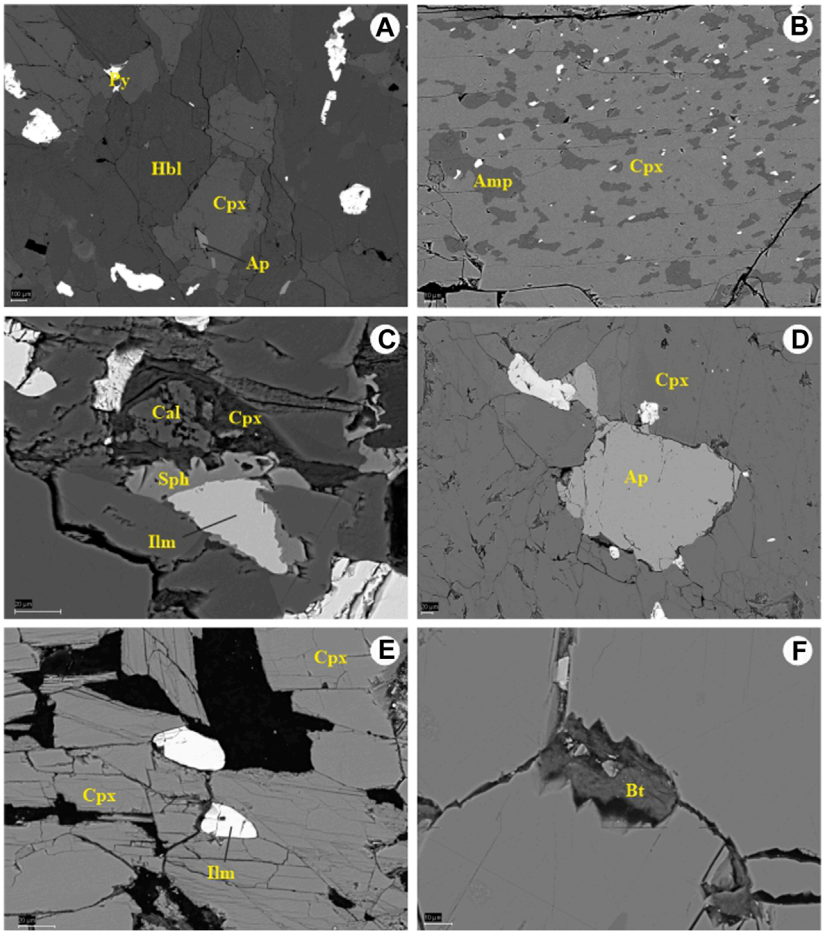

FIGURE 3
Back scattered electron (BSE) images of the studied accessory minerals **(A)** Apatite (Ap) **(B)** Amphiboles (Amp) **(C)** Sphene (Sph) **(D)** Apatite (Ap) **(E)** Ilmenite (Ilm) **(F)** Biotite (Bt) of the Pakkanadu pyroxenites. Abbreviations used: Clinopyroxene (Cpx), Amphibole (Amp), Pyrite (Py), Hornblende (Hbl), Apatite (Ap), Sphene (Sph), Calcite (Cal), Ilmenite (Ilm), Biotite (Bt).

Putirka, 2008). Constraining pressure (P) and temperature (T) of crystallization may decode the evolutionary path of the magma, and thus reveal the possible mineral phases that can coexist (e.g., Thompson, 1974; Botcharnikov et al., 2008). Considering the compositional sensitivity of the major element compositions in the cpx, several empirical cpx-based thermometers and barometers have been developed and calibrated to estimate their P and T of crystallization. In the present study, the abundance of cpx and absence of orthopyroxene (opx) in the pyroxenite samples directed to use single-cpx thermobarometry. WinPyrox program, developed by Yavuz (2013) was employed to calculate the P and T of crystallization. The crystallizing temperatures for the pyroxenites ranges from 905°C to 911°C using the equation of Molin and Zanazzi (1991) based on the diffusive Fe-Mg intracrystalline exchange ordering in cpx. This equation is valid for the magmatic rocks containing cpx only, which is observed in our samples. For the estimation of pressure, we have considered the geobarometry proposed by Nimis and Ulmer (1998), which is firmly suitable for cumulate pyroxenites, and cpx coexisting with basic or ultrabasic melts, respectively. The pressures of crystallization have been estimated to range from 3 Kbar to 9 Kbar.

5 Discussion

5.1 Origin of Pakkanadu pyroxenites

Genesis of different types of pyroxenite rocks, particularly connected with Alaskan-type, layered ultramafic and ophiolitic complexes have been the subject of prime interest in recent times. Alaskan-type complexes frequently coexist with ophiolite complexes exposed along subduction zone boundaries, thrust belts and shear zones (Saleeby, 1992; Thakurta, 2018). Many workers believe that the Alaskan-type complexes are cumulates formed during crystallization of hydrous mafic and ultramafic magmas (e.g., Murray, 1972; Himmelberg and Loney, 1995). Therefore, it is argued that the pyroxenites intruded within the crustal magma chambers, which formed as cumulates and are connected with thick to thin veins or dykes on various scales (Berly et al., 2006). They may also occur as a result of subduction of the oceanic lithosphere, recycling of layers within the subduction zone through mantle convection, and interactions of melts or fluids in the upper mantle (Kornprobst et al., 1990; Pearson et al., 1993).

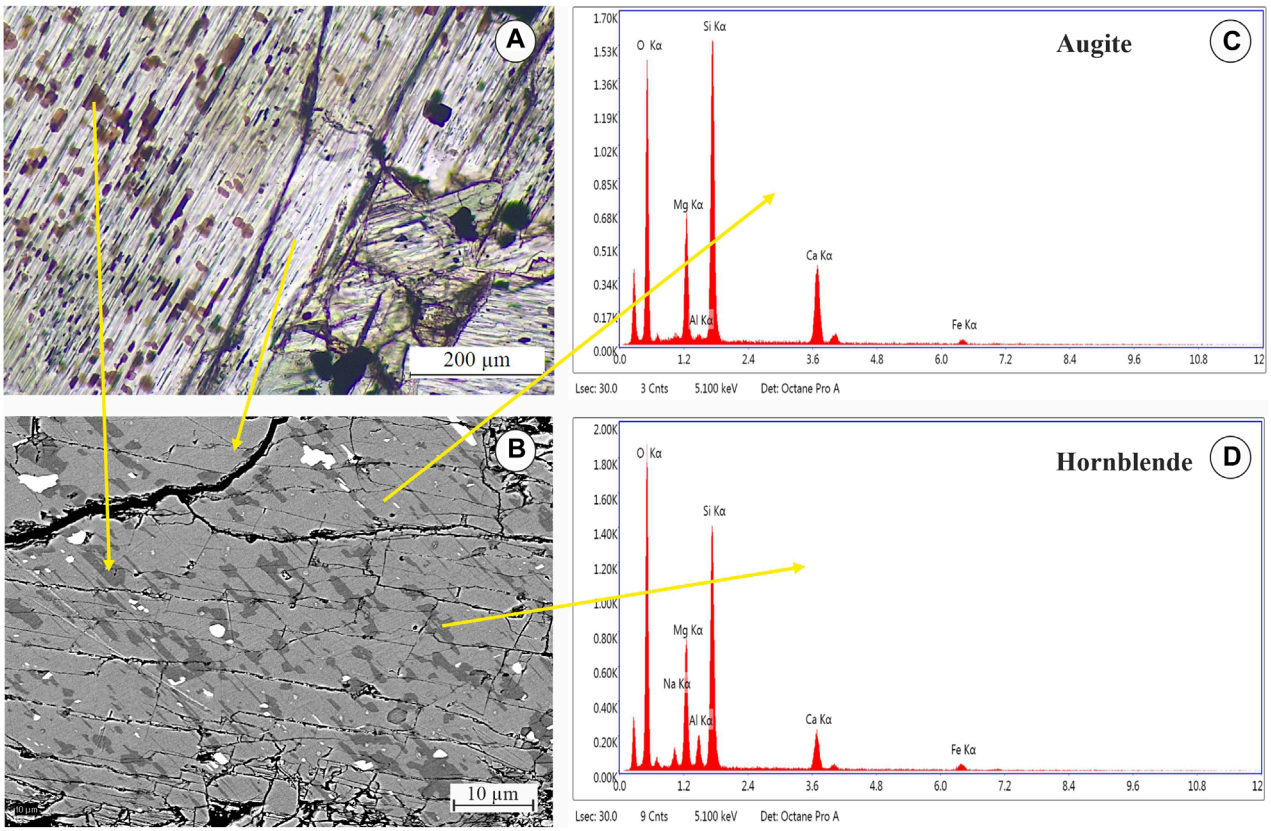

FIGURE 4
(A) Photomicrograph and **(B)** BSE image of the studied pyroxenite samples. **(C)** Energy spectra of **(A)** augite and **(D)** hornblende of the studied pyroxenite samples. Amphiboles are developed over clinopyroxenes is visible as orange blebs in figure **(A)** and dark shades in the BSE image **(B)**.

Cpx from the pyroxenite samples of the present study show a negative correlation between Mg# and TiO_2 plot (Figure 7A) that supports fractional crystallization and thereby formation of cumulates. However, concentration of Cr_2O_3 increases with decreasing Mg# (Figure 7B), which is inconsistent with magmatic differentiation. Moreover, it could be related to the simultaneous crystallization of iron-bearing phases in the intercumulus trapped liquid (Hodges and Papike, 1976). The higher Mg# (76–92) in cpx suggest that they may have evolved as typical Alaskan-type intrusions through crystal fractionation-accumulation processes of a Mg-rich, hydrous parental magma. Such Mg-rich mafic and ultramafic intrusions from a variety of Alaskan-type complexes are known (e.g., Himmelberg and Loney, 1995). The Al_2O_3 content increases with decrease of Mg# in cpx which signifies a typical igneous trend until plagioclase is present in these pyroxenites (Figure 5C). This pattern has previously been seen in pyroxenes from volcanic rocks in the Aleutian arc (Kay and Kay, 1985), lower crustal cumulates (DeBari et al., 1987), the Tonsina ultramafic-mafic assemblage (DeBari and Coleman, 1989), and experimental work on pyroxenites (Müntener et al., 2001). Therefore, this Mg# vs. Al_2O_3 bivariate plot (Figure 5C) for cpx supports the Alaskan-type evolution. The typical occurrence of magnetite in these pyroxenites and other locations is observed in ultramafic complexes worldwide (e.g., Himmelberg et al., 1986; Thakurta, 2018). Tectonic discrimination diagrams based on cpx chemistry, i.e., Ti + Cr vs. Ca and Ti vs. Al_t plots (Figures 8A, B) reveal their formation under an arc tholeiitic environment in subduction zone tectonics (*cf.* Leterrier et al., 1982).

5.2 Magma characterization

Alaskan-type plutonic complexes typically show their association with arc magma chambers and their origin has been linked to cumulate rocks, which have been derived from the crystallization of hydrous mafic and ultramafic magmas (e.g., Irvine, 1974; DeBari and Coleman, 1989; Himmelberg and Loney, 1995). The Pakkanadu pyroxenites have well-preserved cumulate textures and indicate fractional crystallization of the magma.

The Si vs. Al plot of the studied cpx (Figure 9A), which is based on concept that the molecular concentration of SiO_2 in magma determines the amount of silicon in tetrahedral sites of pyroxenes (Kushiro, 1960), a silica under-saturated magma has less silica and is insufficient to fill the tetrahedral site of pyroxenes, therefore, the rest tetrahedral positions are occupied by aluminium and results in a high Al/Si ratio. Whereas, in the case of silica, oversaturated magma, Si is present in excess and occupies the tetrahedral positions in pyroxenes, hence Al/Si ratio is less. Therefore, it suggests that most cpx from Pakkanadu pyroxenites are likely to be crystallized from silica over-saturated magma.

Reaction of melt with cpx to form amp is a widely reported phenomenon in cumulates, mantle pyroxenites, and

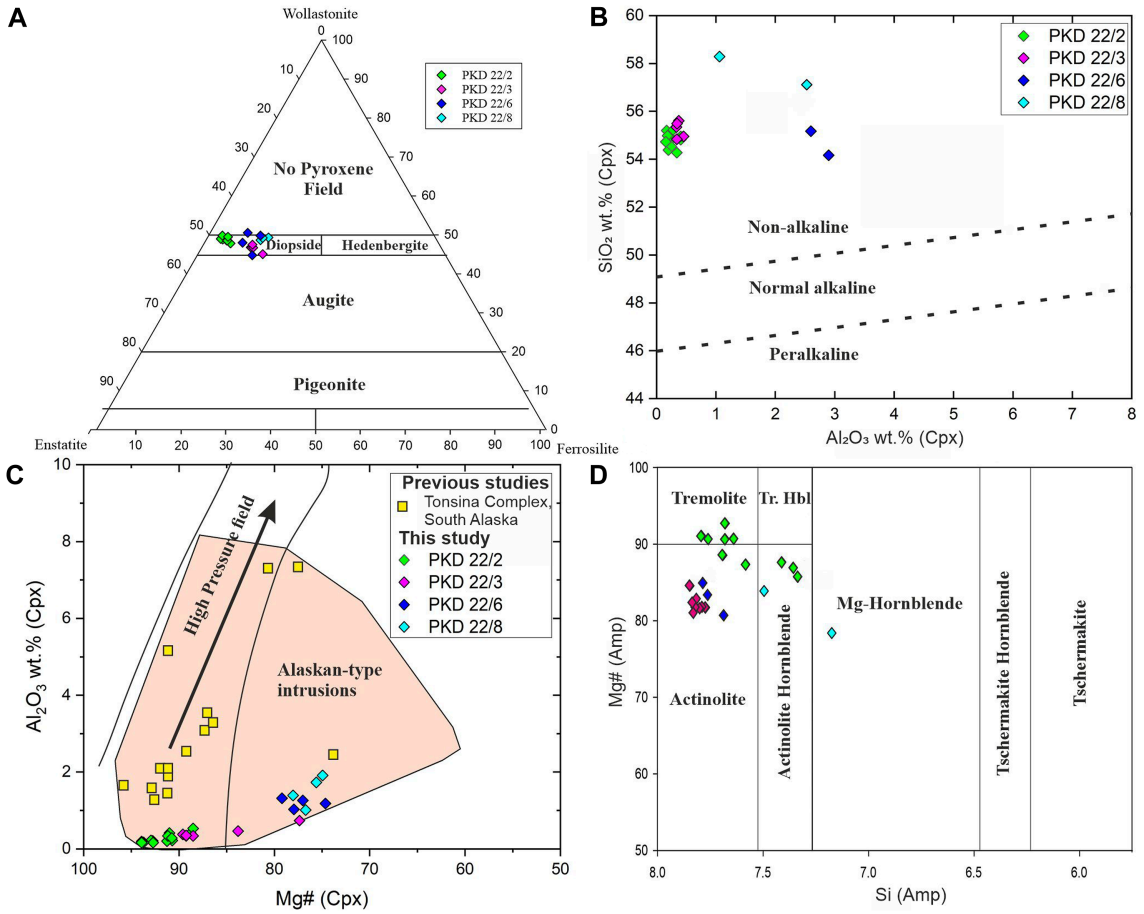

FIGURE 5
(A) Pyroxene ternary classification diagram plotted for pyroxenes from this study (after Morimoto et al., 1988); **(B)** SiO_2 vs. Al_2O_3 diagram plotted for pyroxenes (after Le Bas, 1962); **(C)** Al_2O_3 vs. Mg# variation plot for analysed pyroxene grains showing high pressure and Alaskan-type intrusion field conditions (after Medaris, 1972) and also compared with the previous studies data from Tonsina Complex, South Alaska [Burns (1985); DeBari and Coleman (1989)]. The trend is characterized by an increasing Al_2O_3 content with decreasing Mg# is observed in pyroxenes from volcanic rocks in the Aleutian arc, lower crustal cumulates, the Tonsina ultramafic-mafic assemblage. **(D)** Mg# vs. Si (a.p.f.u) diagram for amphiboles (after Leake et al., 1997), classifying them as Tremolite-Actinolite-Hornblende. Abbreviations used : Cpx - clinopyroxene, Amp - Amphibole.

metasomatized peridotitic mantle (e.g., Best, 1975; Francis, 1976; DeBari et al., 1987; Neal et al., 1988; Coltorti et al., 2004). PKD 22/2 pyroxenite sample shows blebs of brownish orange amp developing over cleavage planes of cpx grains (Figure 4B). These blebs of amp may have developed due to interaction of melt with initially crystallized and settled cpx grains (Smith, 2014). Melt reacting with cpx need not be cogenetic rather may has been formed earlier and progressively replaced with amp by later melt.

Barberi et al. (1971) and Gibb (1973) have stated that Ti content of cpx will be lower if it has crystallized before plagioclase and this provides a confirmation of the first appearance or early crystallization of magnetite. Mineral chemistry of the studied samples have shown the presence of Fe-Ti-O bearing phases, which could be either titano-magnetite or ilmenite. If these phases are early crystallizing, then the mantle source region (i.e., if we generally assume the mantle to be the source of these pyroxenites) should have high oxygen fugacity (fO_2). Moreover, Al^{vi} + 2Ti + Cr vs. Al^{iv}+ Na plot (Figure 9B) confirms that the cpx of present study were crystallised in a highly oxidising environment, which supports the early crystallisation of Fe-Ti-O phases. Kelley and Cottrell (2009) have linked the high fO_2 (oxidizing condition) of the mantle to enrichment by slab-derived fluid-mobile incompatible trace elements (metasomatism) as a result of subduction (Kelley and Cottrell, 2012; Brounce et al., 2014). Therefore, the studied samples have high fO_2 values which indicate an enriched mantle source.

The cpx from the Pakkanadu pyroxenites show negative Nb-Ta anomaly (Figure 6A), which could be linked to arc related magmas. However, U, Th, Rb, Ba and Li in cpx show positive anomalies in all pyroxenite samples except PKD 22/6, which shows negative anomalies for U, and Th, and comparatively low normalized values for Rb and Ba (Figure 6A). PKD 22/2 shows the highest U, Th, Rb, and Ba normalized values, followed by PKD 22/8, PKD 22/3, and least in PKD 22/6. The relative variation of these elements suggests that PKD 22/6 is heavily affected by hydrothermal alteration while PKD 22/2, PKD 22/3 and PKD 22/8 are least affected. This is also consistent with petrographic observations, where PKD 22/2 exhibits initial signature of alteration as amp are found along the grain boundaries and cleavage planes of cpx, while PKD 22/6 shows

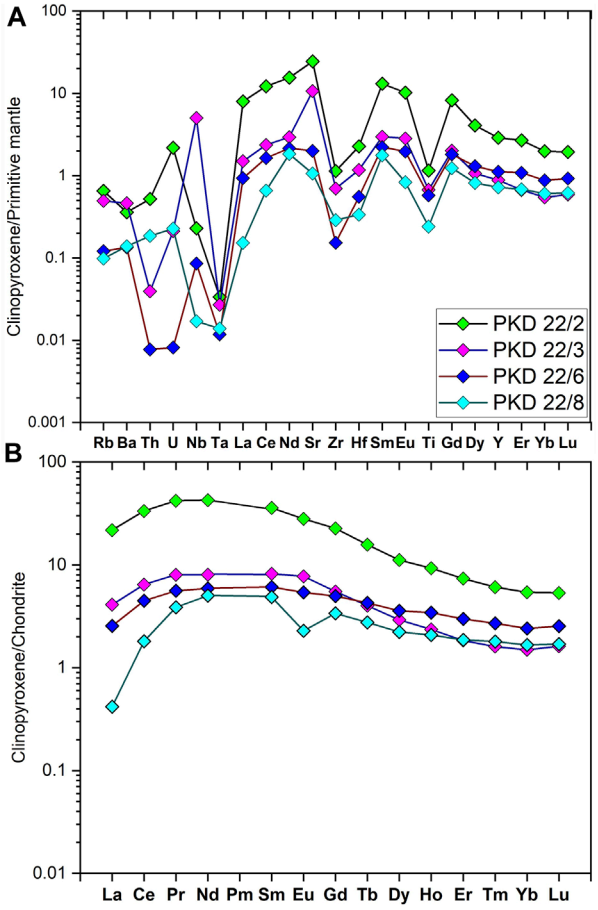

FIGURE 6
(A) Primitive mantle normalized multi-element spidergram for the clinopyroxenes, and **(B)** Chondrite normalized REE pattern. Chondrite normalizing values has been taken from McDonough and Sun (1995), whereas Primitive mantle normalizing values has been taken from Sun and McDonough (1989).

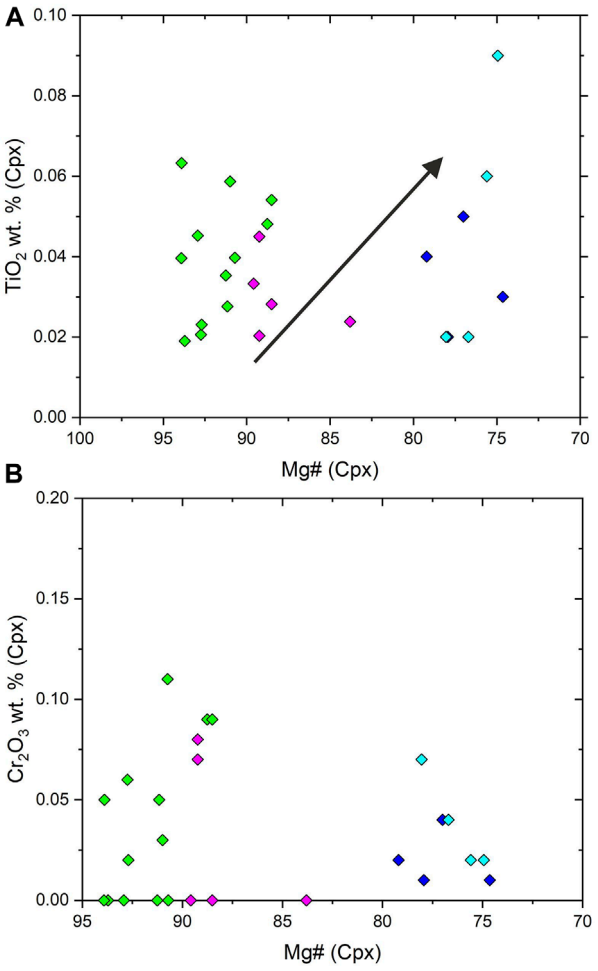

FIGURE 7
(A) TiO_2 vs. Mg# and **(B)** Cr_2O_3 vs. Mg# diagrams for the clinopyroxenes from the Pakkanadu pyroxenites.

highest modal abundance of amp among all the samples. Hence, Nb-Ta anomaly is linked to arc magmas or maybe possibly related to an enriched mantle source.

Enrichment in large-ion lithophile elements (LILEs) and depletion in high-field strength elements (HFSEs) are characteristic of arc magmas generated from enriched mantle sources (e.g., Tatsumi et al., 1986; McCulloch and Gamble, 1991; Arculus, 1994; Hawkesworth et al., 1994). Cpx from the Pakkanadu pyroxenites exhibit enrichment in incompatible elements (U, Sr, La, Ce) and depletion in Ti-Zr-Hf. A few incompatible elements, such as Rb, Ba and Th, are more enriched; however, PKD 22/6 shows depletion in these elements, which could be due to higher hydrothermal alteration causing mobilisation of these elements from cpx to alteration products. Nevertheless, the observed enrichment in incompatible elements and depletion in Ti-Zr-Hf can also be due to crustal contamination. However, mineral chemistry and oxygen fugacity analysis of cpx suggest an enriched mantle source for the magma from which they were crystallised. Therefore, the observed anomalies can be associated to a subduction modified metasomatized mantle source with the presence of phases like rutile (in which Ti-Zr-Hf are compatible). This is also supported by negative Nb-Ta anomaly as these elements are also compatible in rutile.

The Rb-Sr isochron of pyroxenites in the Sevattur alkaline complex along the DRZ shows a concordant age of 773 ± 13 Ma and an initial strontium ratio of 0.70536, which indicates an enriched mantle source (*cf.* Kumar and Gopalan, 1991). Therefore, Sevattur pyroxenites are derived from an enriched mantle source. The Pakkanadu pyroxenites are emplaced along the same DRZ at ca. 763 ± 61 (U-Th-Pb CHIME thorianite dating; Bhagat et al., 2021) might also bear the same magma source. This inference is in accordance with the mineral chemistry and trace element data of cpx which shows variation consistent with rocks generated from a metasomatized mantle.

5.3 Depth of crystallization

The crystallisation history of pyroxenites formed in arc cumulate settings is mostly dependent on the Mg# of the pyroxenes and will help to unravel the processes of its formation. The high Mg# of cpx in the ultramafic cumulates demonstrate the incompatibility

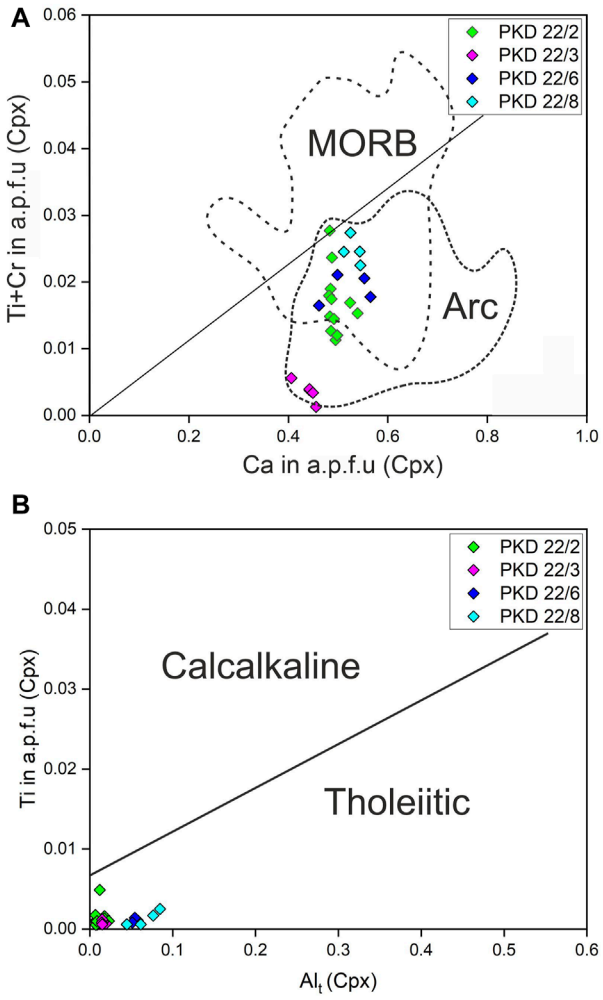

FIGURE 8
(A) Ti + Cr (a.p.f.u) vs. Ca (a.p.f.u) plot (after Leterrier et al., 1982) of cpx grains displaying Arc-like signatures. **(B)** Al$_t$ vs. Ti plot showing tholeiitic nature of the studied cpx grains (after Leterrier et al., 1982).

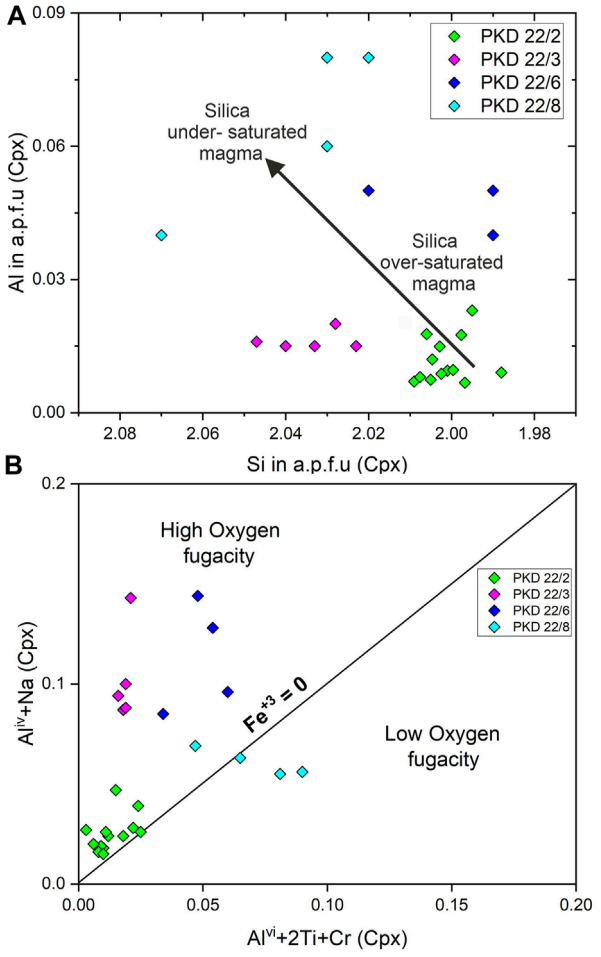

FIGURE 9
(A) Al (a.p.f.u) vs. Si (a.p.f.u) plot of cpx grains discriminating between Silica under-saturated and silica over-saturated nature of the magma (Kushiro, 1960). **(B)** Al$_{iv}$ + Na (a.p.f.u) vs. Al$_{iv}$ + 2Ti + Cr (a.p.f.u) plot (after Schweitzer et al., 1978) of cpx grains showing the high and low oxygen fugacity condition for the magma.

of crystallization in low-pressure conditions. Having un-zoned and compositionally homogeneous cpx in cumulus and inter-cumulus minerals may indicate slow cooling in the magma chamber of the Pakkanadu pyroxenites. Flower et al. (1977) suggested slow cooling and un-zoned minerals may occur in a high-pressure crystallization environment. Lofgren et al. (1974) and Donaldson et al. (1975) have shown that fast cooling rates favour entry of Ti, Ca, Fe, and Al into the pyroxene lattice. These pyroxenes have a low concentration of Ti, which is suggestive of slow cooling rate. Similar results, as evident from the Mg# vs. Al_2O_3 plot (Figure 5C), are obtained for cpx of the Pakkanadu pyroxenites, which suggest their crystallisation in a high-pressure environment (*cf.* Medaris, 1972).

Pakkanadu pyroxenites occur as intrusive, and their interaction with the host alkaline and ultramafic rocks suggests that the mantle underwent effective melt channelization and segregation processes prior to crystallization. Petrographic studies (Figures 2A, B) show cumulate textures and significant levels of shearing. The cpx typically have Mg# values between 76 and 92, which distinguish them as formed in equilibrium with mantle partial melts by fractional crystallization. The absence of aluminous mineral phases does not necessarily indicate that the parental melts were aluminium poor rather; it indicates that the cotectic fraction of aluminium was low at the pressure and temperature at which the pyroxenites crystallized. The high aluminium contents in the cpx suggest that they crystallized from melts with high aluminium content, which are typical of high-pressure cumulates. These pyroxenites crystallize at temperatures between 905 and 911 °C and pressures between 3 and 9 kbar, which is lower to temperatures between 1022 and 1088 °C reported for the wehrlite and 900 °C for olivine, coupled with similar pressures between 9.8 and 10.6 Kbar for the evolution of clinopyroxenes (Maitra et al., 2006). Highly extracted magnesian melts are responsible for the generation of these pyroxenite cumulates and wehrlites under the pressure of 15 Kbar formed at shallower levels near the base of the crust (Maitra et al., 2006).

6 Conclusion

- Pyroxenites of the Pakkanadu alkaline-ultramafic complex contain primarily clinopyroxenes and amphiboles with minor accessory phases like Fe-oxides, sphene and pyrites. Amphiboles are the products of hydrothermal alteration of clinopyroxenes and are secondary in origin.
- Petrography and mineral chemistry of clinopyroxenes reveal that these pyroxenites are cumulates crystallised from a tholeiitic arc-related magma at 905 to 911°C under moderate to high pressure of 3–9 Kbar pressure conditions.
- The geochemical signature of Sevattur pyroxenites emplaced along DRZ suggests a metasomatized mantle source similar to the studied Pakkanadu pyroxenites, which are evident from the trace element patterns (enrichment in incompatible trace elements and depletion in Nb-Ta-Ti-Zr-Hf) and oxygen fugacity studies in clinopyroxenes.
- The Pakkanadu pyroxenites show the Alaskan type magmatism along the DRZ, similar to the adjacent Salem mafic-ultramafic complex and generated from a metasomatized mantle source.

Data availability statement

The original contributions presented in the study are included in the article/Supplementary Material, further inquiries can be directed to the corresponding author.

Author contributions

JP: Conceptualization, Data curation, Formal Analysis, Investigation, Methodology, Validation, Visualization, Writing–original draft, Writing–review and editing. AA: Data curation, Investigation, Writing–original draft, Writing–review and editing. PJ: Data curation, Writing–review and editing. FV: Funding acquisition, Resources, Writing–review and editing. RKS: Conceptualization, Funding acquisition, Investigation, Project administration, Resources, Supervision, Validation, Visualization, Writing–review and editing. HU: Formal Analysis, Writing–review and editing.

Funding

The author(s) declare that no financial support was received for the research, authorship, and/or publication of this article.

Acknowledgments

JP acknowledges the granting of a postdoctoral fellowship from the South African National Research Foundation. FV acknowledges funding from the South African Department of Science and Innovation through their Research Chairs Initiative, as administered by the National Research Foundation (grant number 64779). RKS and AA thank the head of the Department of Geology, Banaras Hindu University for extending the necessary facilities to carry out this project. NV Chalapathi Rao is thanked for his kind access for carrying out the scanning electron microscopy and electron probe microanalysis.

Conflict of interest

The authors declare that the research was conducted in the absence of any commercial or financial relationships that could be construed as a potential conflict of interest.

Publisher's note

All claims expressed in this article are solely those of the authors and do not necessarily represent those of their affiliated organizations, or those of the publisher, the editors and the reviewers. Any product that may be evaluated in this article, or claim that may be made by its manufacturer, is not guaranteed or endorsed by the publisher.

Supplementary material

The Supplementary Material for this article can be found online at: https://www.frontiersin.org/articles/10.3389/feart.2024.1253632/full#supplementary-material

Supplementary Table 1
Results of individual point analyses of the clinopyroxene grains.

Supplementary Table 2
Results of individual point analyses of the amphibole grains.

Supplementary Table 3
Trace element raw data of clinopyroxenes along with standards for reference.

References

Arculus, R. J. (1994). Aspects of magma genesis in arcs. *Lithos* 33 (1-3), 189–208. doi:10.1016/0024-4937(94)90060-4

Barberi, F., Bizouard, H., and Varet, J. (1971). Nature of the clinopyroxene and iron enrichment in alkalic and transitional basaltic magmas. *Contributions Mineralogy Petrology* 33 (2), 93–107. doi:10.1007/bf00386108

Batanova, V. G., Pertsev, A. N., Kamenetsky, V. S., Ariskin, A. A., Mochalov, A. G., and Sobolev, A. V. (2005). Crustal evolution of island-arc ultramafic magma, Galmoenan pyroxenite–dunite plutonic complex, Koryak Highland (Far East Russia). *J. Petrology* 46 (7), 1345–1366. doi:10.1093/petrology/egi018

Berly, T. J., Hermann, J., Arculus, R. J., and Lapierre, H. (2006). Supra-subduction zone pyroxenites from san jorge and santa isabel (Solomon Islands). *J. Petrology* 47 (8), 1531–1555. doi:10.1093/petrology/egl019

Bernard, A., and Ionov, D. A. (2013). Melt– and fluid–rock interaction in supra-subduction lithospheric mantle, evidence from andesite-hosted veined peridotite xenoliths. *J. Petrology* 54, 2339–2378. doi:10.1093/petrology/egt050

Best, M. G. (1975). Amphibole–bearing cumulate inclusions, Grand Canyon, Arizona and their bearing on silica-undersaturated hydrous magmas in the upper mantle. *J. Petrology* 16, 212–236. doi:10.1093/petrology/16.1.212

Bhagat, S., Pandit, D., Srivastava, R. K., and Zakaulla, S. (2021). Chemical microprobe dating of thorianite in carbonatite from the Pakkanadu alkaline-carbonatite complex, Northern Granulite Terrain, Tamil Nadu, India. *Explor. Res. Atomic Minerals (EARFAM)* 29, 145–155.

Bhaskar Rao, Y. J. (2003). Sm-Nd model ages and Rb-Sr isotopic systematics of charnockite gneisses across the Cauvery shear zone, southern India. Implications to the archean-neoproterozoic Terrane boundary in the southern granulite terrain. *Geol. Soc. India Memoirs* 50, 297–317.

Botcharnikov, R. E., Almeev, R. R., Koepke, J., and Holtz, F. (2008). Phase relations and liquid lines of descent in hydrous ferrobasalt – implications for the skaergaard intrusion and columbia river flood basalts. *J. Petrology* 49, 1687–1727. doi:10.1093/petrology/egn043

Bouilhol, P., Schaltegger, U., Chiaradia, M., Ovtcharova, M., Stracke, A., Burg, J.-P., et al. (2011). Timing of juvenile arc crust formation and evolution in the Sapat Complex (Kohistan–Pakistan). *Chem. Geol.* 280 (3-4), 243–256. doi:10.1016/j.chemgeo.2010.11.013

Brounce, M. N., Kelley, K. A., and Cottrell, E. (2014). Variations in Fe3+/Σ Fe of Mariana Arc basalts and mantle wedge f O2. *J. Petrology* 55 (12), 2513–2536. doi:10.1093/petrology/egu065

Burns, L. E. (1985). The Border Ranges ultramafic and mafic complex, south-central Alaska: cumulate fractionates of island-arc volcanics. *Can. J. Earth Sci.* 22 (7), 1020–1038. doi:10.1093/petrology/egu065

Chetty, T. R. K. (2017). *Proterozoic orogens of India, A critical window to Gondwana*. Amsterdam: Elsevier Publications, 426p.

Clark, C., Collins, A. S., Timms, N. E., Kinny, P. D., Chetty, T. R. K., and Santosh, M. (2009). SHRIMP U–Pb age constraints on magmatism and high-grade metamorphism in the Salem Block, southern India. *Gondwana Res.* 16 (1), 27–36. doi:10.1016/j.gr.2008.11.001

Collins, A. S., Clark, C., and Plavsa, D. (2014). Peninsular India in gondwana, the tectonothermal evolution of the southern granulite terrain and its gondwanan counterparts. *Gondwana Res.* 25 (1), 190–203. doi:10.1016/j.gr.2013.01.002

Coltorti, M., Beccaluva, L., Bonadiman, C., Faccini, B., Ntaflos, T., and Siena, F. (2004). Amphibole genesis via metasomatic reaction with clinopyroxene in mantle xenoliths from Victoria Land, Antarctica. *Lithos* 75 (1–2), 115–139. doi:10.1016/j.lithos.2003.12.021

Condie, K. C., Philip, A., and Narayana, B. L. (1982). Geochemistry of the Archean low-to high-grade transition zone, southern India. *Contributions Mineralogy Petrology* 81, 157–167. doi:10.1007/bf00371293

DeBari, S., Kay, S. M., and Kay, R. W. (1987). Ultramafic xenoliths from adagdak volcano, adak, aleutian islands, Alaska, deformed igneous cumulates from the moho of an island arc. *J. Geol.* 95, 329–341. doi:10.1086/629133

DeBari, S. M., and Coleman, R. G. (1989). Examination of the deep levels of an island arc, Evidence from the Tonsina ultramafic-mafic assemblage, Tonsina, Alaska. *J. Geophys. Res.* 10 (B4), 4373–4391. doi:10.1029/jb094ib04p04373

Donaldson, C. H., Usselman, T. M., Williams, R. J., and Lofgren, G. E. (1975). Experimental modeling of the cooling history of Apollo 12 olivine basalts. *Proc. Lunar Sci. Conf.* 6th, 843–870.

Downes, H. (2007). Origin and significance of spinel and garnet pyroxenites in the shallow lithospheric mantle, Ultramafic massifs in orogenic belts in Western Europe and NW Africa. *Lithos* 99 (1–2), 1–24. doi:10.1016/j.lithos.2007.05.006

Drury, S. A., Harris, N. B., Holt, R. W., Reeves-Smith, G. J., and Wightman, R. T. (1984). Precambrian tectonics and crustal evolution in South India. *J. Geol.* 92, 3–20. doi:10.1086/628831

Flower, M. F. J., Robinson, P. T., Schmincke, H. U., and Ohnmacht, W. (1977). Magma fractionation systems beneath the mid-atlantic ridge at 36–37° N. *Contributions Mineralogy Petrology* 64 (2), 167–195. doi:10.1007/bf00371510

Francis, D. M. (1976). The origin of amphibole in lherzolite xenoliths from Nunivak Island, Alaska. *J. Petrol.* 17 (3), 357–378.

Garrido, C. J., Bodinier, J. L., Dhuime, B., Bosch, D., Chanefo, I., Bruguier, O., et al. (2007). Origin of the island arc Moho transition zone via melt-rock reaction and its implications for intracrustal differentiation of island arcs: evidence from the Jijal complex (Kohistan complex, northern Pakistan). *Geology* 35 (8), 683–686. doi:10.1130/g23675a.1

Geological Survey of India (1994). *Geological map of southern peninsular Shield*. Bangalore: Project- Vasundara, AMSE wing, 73p.

Ghosh, J. G., Maarten, J. D., and Zartman, R. E. (2004). Age and tectonic evolution of Neoproterozoic ductile shear zones in the Southern Granulite Terrain of India, with implications for Gondwana studies. *Tectonics* 23, TC3006. doi:10.1029/2002tc001444

Gibb, F. G. F. (1973). The zoned clinopyroxenes of the Shiant Isles sill, Scotland. *J. Petrology* 2, 203–230. doi:10.1093/petrology/14.2.203

Gopalakrishnan, K. (1993). Supportive field evidence for Dharmapuri suture rift zone, Tamil Nadu. *Rec. Geol. Surv. India* 126 (5), 141–145.

Gopalakrishnan, K. (2001). A palaeo-Andean type margin within southern granulite terrain, India. *Geol. Surv. India Special Publ.* 55, 85–96.

Hawkesworth, C., Gallagher, K., Hergt, J., and McDermott, F. (1993). Mantle and slab contributions in ARC magmas. *Annu. Rev. Earth Planet. Sci.* 21, 175–204. doi:10.1146/annurev.ea.21.050193.001135

Hawkesworth, C. J., Gallagher, K., Hergt, J. M., and McDermott, F. (1994). Destructive plate margin magmatism, Geochemistry and melt generation. *Lithos* 33 (1-3), 169–188. doi:10.1016/0024-4937(94)90059-0

Helmy, H. M., Abd El-Rahman, Y. M., Yoshikawa, M., Shibata, T., Arai, S., Tamura, A., et al. (2014). Petrology and Sm–Nd dating of the Genina Gharbia Alaskan-type complex (Egypt), insights into deep levels of Neoproterozoic Island arcs. *Lithos* 198, 263–280. doi:10.1016/j.lithos.2014.03.028

Helmy, H. M., and El Mahallawi, M. M. (2003). Gabbro akarem mafic-ultramafic complex, eastern desert, Egypt, A late precambrian analogue of alaskan-type complexes. *Mineralogy Petrology* 77, 85–108. doi:10.1007/s00710-001-0185-9

Himmelberg, G. R., and Loney, R. A. (1995). *Characteristics and petrogenesis of Alaskan-type ultramafic-mafic intrusions, southeastern Alaska*. Valley Drive Reston: US Geological Survey Professional.

Himmelberg, G. R., Loney, R. A., and Craig, J. T. (1986). *Petrogenesis of the ultramafic complex at the Blashke Islands, southeastern Alaska*. Alexandria, VA: Department of the Interior, US Geological Survey bulletin.

Hirschmann, M. M., Kogiso, T., Baker, M. B., and Stolper, E. M. (2003). Alkalic magmas generated by partial melting of garnet pyroxenite. *Geology* 31, 481–484. doi:10.1130/0091-7613(2003)031<0481:amgbpm>2.0.co;2

Hirschmann, M. M., and Stolper, E. M. (1996). A possible role for garnet pyroxenite in the origin of the 'garnet signature' in MORB. *Contributions Mineralogy Petrology* 124, 185–208. doi:10.1007/s004100050184

Hodges, F. N., and Papike, J. J. (1976). DSDP site 334, magmatic cumulates from oceanic layer 3. *J. Geophys. Res.* 81 (23), 4135–4151. doi:10.1029/jb081i023p04135

Irvine, T. N. (1974). *Petrology of the Duke Island ultramafic complex southeastern Alaska*.

Jagoutz, O., Müntener, O., Ulmer, P., Pettke, T., Burg, J.-P., Dawood, H., et al. (2007). Petrology and mineral chemistry of lower crustal intrusions: the chilas complex, kohistan (NW Pakistan). *J. Petrology* 48 (10), 1895–1953. doi:10.1093/petrology/egm044

Kay, S. M., and Kay, R. W. (1985). Role of crystal cumulates and the oceanic crust in the formation of the lower crust of the Aleutian arc. *Geology* 13, 461–464. doi:10.1130/0091-7613(1985)13<461:roccat>2.0.co;2

Kelemen, P. B. (1990). Reaction between ultramafic rock and fractionating basaltic magma I. Phase relations, the origin of calc-alkaline magma series, and the formation of discordant dunite. *J. Petrology* 31, 51–98. doi:10.1093/petrology/31.1.51

Kelley, K. A., and Cottrell, E. (2009). Water and the oxidation state of subduction zone magmas. *Science* 325, 605–607. doi:10.1126/science.1174156

Kelley, K. A., and Cottrell, E. (2012). The influence of magmatic differentiation on the oxidation state of Fe in a basaltic arc magma. *Earth Planet. Sci. Lett.* 329, 109–121. doi:10.1016/j.epsl.2012.02.010

Kogiso, T., Hirschmann, M. M., and Frost, D. J. (2003). High-pressure partial melting of garnet pyroxenite, possible mafic lithologies in the source of ocean island basalts. *Earth Planet. Sci. Lett.* 216, 603–617. doi:10.1016/s0012-821x(03)00538-7

Kogiso, T., Hirschmann, M. M., and Pertermann, M. (2004). High pressure partial melting of mafic lithologies in the mantle. *J. Petrology* 45, 2407–2422. doi:10.1093/petrology/egh057

Kornprobst, J., Piboule, M., Roden, M., and Tabit, A. (1990). Corundum-bearing garnet clinopyroxenites at Beni Bousera (Morocco), original plagioclase-rich gabbros recrystallized at depth within the mantle. *J. Petrology* 31 (3), 717–745. doi:10.1093/petrology/31.3.717

Kostopoulos, D., and Murton, B. (1992). "Origin and distribution of components in boninite genesis, significance of the OIB component," in *Ophiolites and their modern oceanic analogues*. Editors L. M. Parson, B. J. Murton, and P. Browning (London: Geological Society, London, Special Publications), 133–154.

Kumar, A., and Gopalan, K. (1991). Precise Rb-Sr age and enriched mantle source of the Sevattur carbonatites, Tamil Nadu, South India. *Curr. Sci.* 60 (11), 653–655.

Kumar, A., Nirmal, C. S., Gopalan, K., and Macdougall, J. D. (1998). A long-lived enriched mantle source for two Proterozoic carbonatite complexes from Tamil Nadu, southern India. *Geochimica Cosmochimica Acta* 62 (3), 515–523. doi:10.1016/s0016-7037(97)00341-4

Kushiro, I. (1960). Si-Al relation in clinopyroxenes from igneous rocks. *Am. J. Sci.* 258 (8), 548–554. doi:10.2475/ajs.258.8.548

Kutty, T. R. N., Murthy, S. R. N., and Anantha, I. G. V. (1986). REE geochemistry and petrogenesis of ultramafic rocks of Chalk Hills, Salem. *J. Geol. Soc. India* 28 (6), 449–466.

Lambart, S., Laporte, D., Provost, A., and Schiano, P. (2012). Fate of pyroxenite-derived melts in the peridotitic mantle, thermodynamic and experimental constraints. *J. Petrology* 53, 451–476. doi:10.1093/petrology/egr068

Leake, B. E., Woolley, A. R., Arps, C. E. S., Birch, W. D., Gilbert, M. C., Grice, J. D., et al. (1997). Nomenclature of amphiboles, report of the subcommittee on amphiboles of the international mineralogical association, commission on new minerals and mineral names. *Can. Mineral.* 35 (1), 219–246. doi:10.1180/minmag.1997.061.405.13

Le Bas, M. J. (1962). The role of aluminum in igneous clinopyroxenes with relation to their parentage. *Am. J. Sci.* 260 (4), 267–288. doi:10.2475/ajs.260.4.267

Leterrier, J., Maury, R. C., Thonon, P., Girard, D., and Marchal, M. (1982). Clinopyroxene composition as a method of identification of the magmatic affinities of paleo-volcanic series. *Earth Planet. Sci. Lett.* 59, 139–154. doi:10.1016/0012-821x(82)90122-4

Lofgren, G. E., Donaldson, C. H., Williams, R. J., Mullins, O., and Usselman, T. M. (1974) Experimentally reproduced textures and mineral chemistry of Apollo 15 quartz normative basalts. Proceedings of the Lunar Science 5th Conference. New York. (Pergamon Press, Inc) 549–567.

Maitra, M., Bose, M. K., and Ray, J. (2006). Interpretative mineral chemistry of ultramafic rocks of Chalk Hills, Tamil Nadu. *Geol. Soc. India* 68 (5), 831–840.

McCulloch, M. T., and Gamble, J. A. (1991). Geochemical and geodynamical constraints on subduction zone magmatism. *Earth Planet. Sci. Lett.* 102, 358–374. doi:10.1016/0012-821x(91)90029-h

McDonough, W. F., and Sun, S. (1995). The composition of the Earth. *Chem. Geol.* 120 (3–4), 223–253. doi:10.1016/0009-2541(94)00140-4

Medaris, L. G., Beard, B. L., Johnson, C. M., Valley, J. W., Spicuzza, M. J., Jelínek, E., et al. (1995). Garnet pyroxenite and eclogite in the Bohemian Massif, geochemical evidence for Variscan recycling of subducted lithosphere. *GeologischeRundschau* 84, 489–505. doi:10.1007/s005310050020

McInnes, B. I., Gregoire, M., Binns, R. A., Herzig, P. M., and Hannington, M. D. (2001). Hydrous metasomatism of oceanic sub-arc mantle, Lihir, Papua New Guinea: petrology and geochemistry of fluid-metasomatised mantle wedge xenoliths. *Earth Planet. Sci. Lett.* 188(1-2), 169–183.

Medaris, L. G., Jr (1972). High-pressure peridotites in southwestern Oregon. *Geol. Soc. Am. Bull.* 83 (1), 41–58. doi:10.1130/0016-7606(1972)83[41:hpiso]2.0.co;2

Mercier, J.-C. C. (1980). Single pyroxene thermobarometry. *Tectonophysics* 70, 1–37. doi:10.1016/0040-1951(80)90019-0

Miyazaki, T., Kagami, H., Shuto, K., Morikiyo, T., Ram Mohan, V., and Rajasekaran, K. C. (2000). Rb Sr geochronology, Nd-Sr isotopes, and whole rock geochemistry of Yelagiri and Sevattur syenites, Tamil Nadu, south India. *Gondwana Res.* 3 (1), 39–53. doi:10.1016/s1342-937x(05)70056-3

Molin, G., and Zanazzi, F. (1991). Intracrystalline Fe2+-Mg ordering in augite: experimental study and geothermometric applications. *Eur. J. Mineralogy* 3, 863–875. doi:10.1127/ejm/3/5/0863

Moller, A., Geisler, T., Scheicher, H., Todt, W., Viladakar, S. G., and Subramanian, V. (2001). "Inter-relationship between carbonatite-pyroxenite-syenite complexes of southern India," in *Symposium of carbonatites and associated alkaline rocks and field workshop on carbonatites of Tamil Nadu*, Chennai, India, 15–16.

Morimoto, N. (1988). Die nomenklatur von Pyroxenen. *Mineralogy Petrology* 39 (1), 55–76. doi:10.1007/bf01226262

Müntener, O., Kelemen, P. B., and Grove, T. L. (2001). The role of H 2 O during crystallization of primitive arc magmas under uppermost mantle conditions and genesis of igneous pyroxenites: an experimental study. *Contributions Mineralogy Petrology* 141, 643–658. doi:10.1007/s004100100266

Muntener, O., and Ulmer, P. (2006). Experimentally derived high pressure cumulates from hydrous arc magmas and consequences for the seismic velocity structure of lower arc crust. *Geophys. Res. Lett.* 33, 1–5. doi:10.1029/2006gl027629

Murray, C. G. (1972). Zoned ultramafic complexes of the Alaskan-type: feeder pipes of andesitic volcanoes. *Geol. Soc. Am.* 132, 313–335.

Naqvi, S. M., and Rogers, J. J. W. (1987). *Precambrian Geology of India*. New York: Oxford University press, 223p.

Neal, C. R. (1988). The origin and composition of metasomatic fluids and amphiboles beneath Malaita, Solomon Islands. *J. Petrology* 29, 149–179. doi:10.1093/petrology/29.1.149

Nimis, P. (1995). A clinopyroxene geobarometer for basaltic systems based on crystal-structure modeling. *Contributions Mineralogy Petrology* 121, 115–125. doi:10.1007/s004100050093

Nimis, P. (1999). Clinopyroxene geobarometry of magmatic rocks. Part 2. Structural geobarometers for basic to acid, tholeiitic and mildly alkaline magmatic systems. *Contributions Mineralogy Petrology* 135, 62–74. doi:10.1007/s004100050498

Nimis, P., and Taylor, W. R. (2000). Single clinopyroxene thermobarometry for garnet peridotites. Part I. Calibration and testing of a Cr-in-Cpx barometer and an enstatite-in-Cpx thermometer. *Contributions Mineralogy Petrology* 139, 541–554. doi:10.1007/s004100000156

Nimis, P., and Ulmer, P. (1998). Clinopyroxene geobarometry of magmatic rocks Part 1, an expanded structural geobarometer for anhydrous and hydrous, basic and ultrabasic systems. *Contributions Mineralogy Petrology* 133, 122–135. doi:10.1007/s004100050442

Noble, J. A. (1960). Correlation of the ultramafic complexes of southeastern Alaska with those of other parts of North America and the world. *Petrogr. Prov. Igneous Metamorph. Rocks*, 188–197.

O'Driscoll, B., and VanTongeren, J. A. (2017). Layered intrusions: from petrological paradigms to precious metal repositories. *Elem. Int. Mag. Mineralogy, Geochem. Petrology* 13 (6), 383–389. doi:10.2138/gselements.13.6.383

Pandit, M. K., Sial, A. N., Sukumaran, G. B., Pimentel, M. M., Ramasamy, A. K., and Ferreira, V. P. (2002). Depleted and enriched mantle sources for Paleo-and Neoproterozoic carbonatites of southern India, Sr, Nd, C–O isotopic and geochemical constraints. *Chem. Geol.* 189 (1-2), 69–89. doi:10.1016/s0009-2541(02)00136-5

Pearson, D. G., Davies, G. R., and Nixon, P. H. (1993). Geochemical constraints on the petrogenesis of diamond facies pyroxenites from the Beni Bousera peridotite massif, North Morocco. *J. Petrology* 34 (1), 125–172. doi:10.1093/petrology/34.1.125

Putirka, K., Johnson, M., Kinzler, R., Longhi, J., and Walker, D. (1996). Thermobarometry of mafic igneous rocks based on clinopyroxene-liquid equilibria, 0-30 kbar. *Contributions Mineralogy Petrology* 123, 92–108. doi:10.1007/s004100050145

Putirka, K. D. (2008). Thermometers and barometers for volcanic systems. *Mineral. Geochem.* 69, 61–120. doi:10.2138/rmg.2008.69.3

Ramakrishnan, M. (1988). Tectonic evolution of the Archean high grade terrain of south India. *J. Geol. Soc. India* 31, 118–119.

Ramakrishnan, M. (1993). Tectonic evolution of granulite terrains of southern India. *Geol. Soc. India* 25, 35–44.

Ramakrishnan, M., and Vaidyanadhan, R. (2010). *Geology of India*. Bangalore: Geological. Society of India, pp994.

Rao, A. T., and Raman, C. V. (1979). Spinel bronzite pyroxenites from Vemparala, Andhra Pradesh. *J. Geol. Soc. India* 20 (3), 142–144.

Renjith, M. L., Santosh, M., Tang, L., Satyanarayanan, M., Korakoppa, M. M., Tsunogae, T., et al. (2016). Zircon U–Pb age, Lu-Hf isotope, mineral chemistry and geochemistry of Sundamalai peralkaline pluton from the Salem Block, southern India, Implications for Cryogenian adakite-like magmatism in an aborted-rift. *J. Asian Earth Sci.* 115, 321–344. doi:10.1016/j.jseaes.2015.10.001

Saitoh, Y., Toshiaki, T., Santosh, M., Chetty, T. R. K., and Kenji, H. (2011). Neoarchean high-pressure metamorphism from the northern margin of the Palghat–Cauvery Suture Zone, southern India, Petrology and zircon SHRIMP geochronology. *J. Asian Earth Sci.* 42 (3), 268–285. doi:10.1016/j.jseaes.2010.11.015

Saleeby, J. B. (1992). Age and tectonic setting of the Duke Island ultramafic intrusion, south-east Alaska. *Can. J. Earth Sci.* 29 (3), 506–522. doi:10.1139/e92-044

Samal, A. K., Rai, A. K., and Srivastava, R. K. (2021). Multiple mantle melting events for two overlapping ca. 2.21-2.18 Ga mafic dyke swarms in the Dharwar craton, India. *Int. Geol. Rev.* 63 (17), 2166–2191. doi:10.1080/00206814.2020.1827460

Samuel, V. O., Santosh, M., Shuwen, L., Wei, W., and Sajeev, V. (2014). Neoarchean continental growth through arc magmatism in the Nilgiri Block, southern India. *Precambrian Res.* 245, 146–173. doi:10.1016/j.precamres.2014.02.002

Santosh, M., Maruyama, S., and Sato, K. (2009). Anatomy of a cambrian suture in gondwana, pacific-type orogeny in southern India? *Gondwana Res.* 16 (2), 321–341. doi:10.1016/j.gr.2008.12.012

Santosh, M., Yang, Q.-Y., Ram Mohan, M., Tsunogae, T., Shaji, E., and Satyanarayanan, M. (2014). Cryogenian alkaline magmatism in the Southern Granulite Terrane, India, Petrology, geochemistry, zircon U–Pb ages and Lu–Hf isotopes. *Lithos* 208, 430–445. doi:10.1016/j.lithos.2014.09.016

Schleicher, H., Kramm, U., Pernicka, E., Schidlowski, M., Schmidt, F., Subramanian, V., et al. (1998). Enriched subcontinental upper mantle beneath southern India, evidence from Pb, Nd, Sr, and C–O isotopic studies on Tamil Nadu carbonatites. *J. Petrology* 39 (10), 1765–1785. doi:10.1093/petroj/39.10.1765

Schweitzer, E. L., Papike, J. J., and Bence, A. E. (1978). Clinopyroxenes from deep sea basalts, A statistical analysis. *Geophys. Res. Lett.* 5, 573–576. doi:10.1029/gl005i007p00573

Sharma, A., Giri, R. K., Rao, N. C., Rahaman, W., Pandit, D., and Sahoo, S. (2019). Arc-related pyroxenites derived from a long-lived Neoarchean subduction system at the southwestern margin of the Cuddapah Basin: geodynamic implications for the evolution of the Eastern Dharwar Craton, southern India. *J. Geol.* 127 (5), 567–591. doi:10.1086/704361

Smith, D. J. (2014). Clinopyroxene precursors to amphibole sponge in arc crust. *Nat. Commun.* 5 (1), 4329–4336. doi:10.1038/ncomms5329

Sobolev, A. V., Hofmann, A. W., Sobolev, S. V., and Nikogosian, I. K. (2005). An olivine-free mantle source of Hawaiian shield basalts. *Nature* 434, 590–597. doi:10.1038/nature03411

Srivastava, R., and Sinha, A. K. (2007). Nd and Sr isotope systematics and geochemistry of a plume-related early cretaceous alkaline-mafic ultramafic igneous complex from Jasra, Shillong plateau, northeastern India. *Geol. Soc. Am.* 430, 815–830. doi:10.1130/2007.2430(37)

Srivastava, R. K., Banerjee, S., Longstaffe, F. J., Bhagat, S., and Sinha, D. K. (2022). Stable isotopic study of carbonatites from the Pakkanadu Alkaline Complex, southern India, Constraints on carbonatite melt evolution and sub-solidus, high temperature fluid-rock interaction. *Lithos* 15 (430-431), 106863. doi:10.1016/j.lithos.2022.106863

Sukumaran, G. B. (1987). *Study of carbonatites and alkaline rocks of mulakkadu and Pakkanadu, Salem district. Degree of doctor of philosophy*. Tamil Nadu, India. September: University of Madras.

Sun, S. S., and McDonough, W. F. (1989). "Chemical and isotopic systematics of oceanic basalts, implications for mantle composition and processes," in *Magmatism in the ocean basins*. Editors A. D. Saunders, and M. J. Norry (London: Geological Society, London, Special Publications), 313–345.

Swaminath, J., Ramakrishnan, M., and Viswanatha, M. N. (1974). "The cratonic greenstone belts of southern Karnataka and their possible relation to the charnockite mobile belt," in *Int. Seminar on tectonics and metallogeny of southeast asia and far east* (Delhi, India: Controller of publications), 11–16.

Tatsumi, Y., Hamilton, D. L., and Nesbitt, R. W. (1986). Chemical characteristics of fluid phase released from a subducted lithosphere and origin of arc magmas, evidence from high pressure experiments and natural rocks. *J. Volcanol. Geotherm. Res.* 29, 293–309. doi:10.1016/0377-0273(86)90049-1

Taylor, J. R. (1960). Origin of the ultramafic complexes in southeastern Alaska. *Petrogr. Prov. Igneous Metamorph. Rocks*, 175–187.

Thakurta, J. (2018). *Alaskan-type complexes and their associations with economic mineral deposits in processes and ore deposits of ultramafic-mafic magmas through space and time*. Elsevier, Amsterdam, pp. 269–302.

Thompson, R. N. (1974). Some high-pressure pyroxenes. *Mineral. Mag.* 39, 768–787. doi:10.1180/minmag.1974.039.307.04

Tilhac, R., Gregoire, M., O'Reilly, S. Y., Griffin, W. L., Henry, H., and Ceuleneer, G. (2017). Sources and timing of pyroxenite formation in the sub-arc mantle, Case study of the Cabo Ortegal Complex, Spain. *Earth Planet. Sci. Lett.* 474, 490–502. doi:10.1016/j.epsl.2017.07.017

Van Achterbergh, E., Ryan, C. G., Jackson, S. E., and Griffin, W. L. (2001). "Data reduction software for LA-ICP-MS," in *Laser ablation-ICP mass spectrometry in the earth sciences, principles and applications*. Editor P. J. Sylvester (Canada: Mining Association of Canada), 239–243.

Xiong, Q., Zheng, J.-P., Griffin, W. L., O'Reilly, S. Y., and Pearson, N. J. (2014). Pyroxenite dykes in orogenic peridotite from North Qaidam (NE Tibet, China) track metasomatism and segregation in the mantle wedge. *J. Petrology* 55 (12), 2347–2376. doi:10.1093/petrology/egu059

Yavuz, F. (2013). WinPyrox, A Windows program for pyroxene calculation classification and thermobarometry. *Am. Mineralogist* 98 (7), 1338–1359. doi:10.2138/am.2013.4292